JMEPEG (2012) 21:995–1002
DOI: 10.1007/s11665-011-9990-4

1059-9495/$19.00

Inhibition of Zinc Corrosion by Some Benzaldehyde Derivatives in HCl Solution

M. Abdallah, I. Zaafarany, A.S. Fouda, and D. Abd El-Kader

(Submitted July 6, 2010; in revised form March 24, 2011)

The effect of some benzaldehyde derivatives on the corrosion of zinc in 0.5 M HCl solution is studied in this article using mass loss, potentiodynamic polarization, and electrochemical impedance spectroscopy (EIS) techniques. The percentage inhibition efficiency (%In) was found to increase with increasing concentration of the inhibitor and with decreasing temperature. Polarization studies indicated that all of the compounds studied are mixed-type inhibitors. The inhibitive action of these benzaldehyde derivatives has been discussed in view of the adsorption on the zinc surface. The adsorption process follows Temkin's isotherm. The addition of KSCN, KI, and KBr to benzaldehyde derivatives has enhanced the inhibition efficiency because of synergistic effect. The mechanism of inhibition process is discussed in the light of the chemical structures of the investigated inhibitors.

Keywords benzaldehyde derivatives, corrosion inhibitors, HCl, synergistic effect, zinc

1. Introduction

Zinc is one of the most widely used metals and is often attacked by aggressive media, such as acids, bases, and salt solutions (Ref 1, 2). For scale removal and cleaning of zinc surface with acid solutions, the use of organic inhibitors is one of the most practical methods for protection against corrosion, especially in acidic media (Ref 3-19).

The corrosion inhibition by organic compounds is connected with their adsorption properties. The role of the adsorbed inhibitor is to isolate the metal from the corrosive medium and/or to modify the electrode reactions which cause dissolution of the metal. The adsorption is ascribed to the effects of aromatic rings which are adsorbed parallel to the metal surface (Ref 20). It has been observed that the adsorption depends mainly on the electronic structure of the molecules, as well as on the surface morphology of the metal (Ref 21, 22).

The aim of this study is to investigate the effect of some benzaldehyde derivatives on the corrosion of Zn in 0.5 M HCl solution using mass loss, potentiodynamic polarization, and electrochemical impedance spectroscopy (EIS) techniques. The effect of temperature on the dissolution of Zn in free and inhibited acid solution was also investigated.

The investigated inhibitors are described in the following:

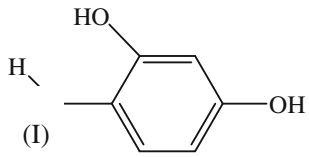

(I)

2,4-dihydroxybenzaldehyde

$C_7H_6O_3$

Mol. Wt.: 138.12

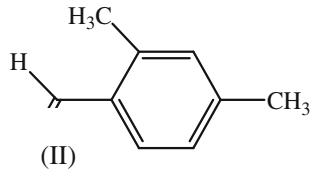

(II)

2,4-dimethyl-benzaldehyde

$C_9H_{10}O$

Mol. Wt.: 134.18

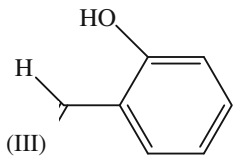

(III)

salicaldehyde 2-hydroxybenzaldehyde

$C_7H_6O_2$

Mol. Wt.: 122.12

2. Experimental

The zinc (BDH grade) sheets used in this investigation have the following chemical composition:

M. Abdallah and **I. Zaafarany**, Department of Chemistry, Faculty of Applied Science, Umm Al-Qura University, Makkah Al Mukaramha, Saudi Arabia; **A.S. Fouda** and **D. Abd El-Kader**, Department of Chemistry, Faculty of Science, El-Mansoura University, El Mansoura 35516, Egypt; and **M. Abdallah**, Department of Chemistry, Faculty of Science, Benha University, Benha, Egypt. Contact e-mails: metwally555@yahoo.com and asfouda@mans.edu.eg.

Element	Pb	Fe	Cd	Cu	Zn
wt.%	0.001	0.002	0.001	0.003	Rest

All the chemicals used were of AR grade and used as received. Specimens of zinc sheets were first polished with different grades of emery papers, to obtain a smooth surface, degreased in acetone in an ultrasonic bath, washed by bidistilled water, and dried between two fitter papers. The solutions of 0.5 M HCl were prepared with bidistilled water.

2.1 Mass-Loss Measurements

For mass-loss measurements, rectangular zinc specimens of size $20 \times 20 \times 2$ mm were immersed in 100-mL inhibited and uninhibited solutions and allowed to remain for several intervals at 30 °C in water thermostat. The percentage inhibition efficiency (%In) of the inhibitor was calculated using the following equation:

$$\%\mathrm{In} = \left[\frac{M_{\mathrm{free}} - M_{\mathrm{inh}}}{M_{\mathrm{free\ pure}}}\right] \times 100 \qquad \text{(Eq 1)}$$

where M_{free} and M_{inh} are the mass losses in the absence and the presence of inhibitors, respectively.

2.2 Potentiodynamic Polarization Measurements

Potentiodynamic polarization studies were carried out on zinc electrode in 0.5 M HCl in the presence and the absence of different concentrations of the inhibitors used at 25 °C and at the scan rate of 10 mV s^{-1}. Saturated calomel electrode was used as reference electrode while a platinum wire as a counter electrode. All the experiments were carried out at 25 ± 0.1 °C. A 1-cm-long cylindrical zinc electrode having a diameter of 1.25 mm was used as working electrode. The %In was calculated from the following equation:

$$\%\mathrm{In} = \left[\frac{I_{\mathrm{corr}} - I_{\mathrm{inh}}}{I_{\mathrm{corr}}}\right] \times 100 \qquad \text{(Eq 2)}$$

where I_{corr} and I_{inh} are the uninhibited and inhibited corrosion current densities, respectively.

2.3 Electrochemical Impedance Spectroscopy (EIS) Method

The EIS experiments were conducted at 298 ± 1 K at the OCP (open circuit potential) over a frequency ranging from 1 kHz to 1 Hz, using a signal amplitude perturbation of 10 mV using potentiostat/galvanostat (Gamry PCI 300/4) and a personal computer with EIS 300 software for calculation. Nyquist plots were obtained from the results of these experiments. Values of the charge transfer resistance (R_{ct}) were obtained from these plots by determining the difference in the values of impedance at low and high frequencies, as suggested by Saliyan and Adhikari (Ref 23). Values of the double-layer capacitance (C_{dl}) were obtained from the following equation:

$$C_{\mathrm{dl}} = \frac{1}{2\pi f_{\mathrm{max}} R_{\mathrm{ct}}} \qquad \text{(Eq 3)}$$

%IE was calculated using the equation:

$$\%\mathrm{In} = \frac{(1/R'_{\mathrm{ct}}) - (1/R_{\mathrm{ct}})}{(1/R'_{\mathrm{ct}})} \times 100 \qquad \text{(Eq 4)}$$

where R'_{ct} and R_{ct} are the charge transfer resistance values in the absence and the presence of the inhibitors, respectively.

3. Results and Discussion

3.1 Mass-Loss Measurements

Figure 1 represents the relation between times and mass loses of Zn coupons in 0.5 M HCl solution devoid of and containing different concentrations of compound I as an example. Similar curves were also obtained for the other two tested compounds (not shown). An inspection of this figure reveals that the linear variation of mass loss with time in the inhibited and uninhibited 0.5 M HCl solution indicates the absence of insoluble films during corrosion i.e., the inhibitors are first adsorbed on the metal surface, which thereafter impede corrosion either by merely blocking the reaction sites (anodic and cathodic) or by altering the mechanism of the anodic and cathodic processes. From a further inspection of Fig. 1, it becomes obvious that the weight loss of Zn samples was decreased. This means that the presence of these derivatives retards the corrosion of Zn in 0.5 M HCl solutions or, in other words, these derivatives act as inhibitors. The values of percentage inhibition of investigated compounds are given in Table 1. From this table, it is clear that the %In of these compounds increases with increasing concentration of these additives. The order of the inhibition efficiency of benzaldehyde decreases in following manner: compound (I) > compound (II) > compound (III).

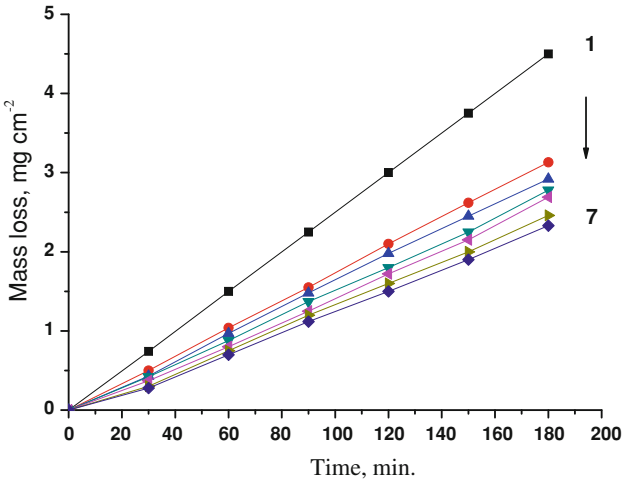

Fig. 1 Mass loss-time curves for zinc dissolution in 0.5 M HCl in the absence and the presence of different concentrations of inhibitors (I) at 30 °C: (1) 0.00 M compound I, (2) 1×10^{-6}, (3) 3×10^{-6}, (4) 5×10^{-6}, (5) 7×10^{-6}, (6) 9×10^{-6}, and (7) 11×10^{-6} M

Table 1 Effect of inhibitors concentrations on the percentage inhibition efficiency (%In) of zinc in 0.5 M HCl solution from mass-loss method at 30 °C

	%In		
Concentration, M	**(I)**	**(II)**	**(III)**
1×10^{-6}	30.3	28.3	26.2
3×10^{-6}	35.1	31.6	28.3
5×10^{-6}	38.2	36.2	32.5
7×10^{-6}	40.1	38.1	35.5
9×10^{-6}	45.2	44.3	40.1
11×10^{-6}	48.3	46.1	42.2

3.2 Synergistic Effect

The %In of the tested derivatives is low, and hence, in order to increase these values, we use KI, KSCN, and KBr in addition to the different concentrations of the investigated derivatives. The effect of KI, KSCN, and KBr on the performance of benzaldehyde derivatives has been studied using mass-loss technique. Similar curves as those in Fig. 1 were obtained (not shown). The values of IE for specific concentration of KI, KSCN, and KBr (1×10^{-2} M) in the presence of various concentrations of inhibitors are given in Table 2.

It is seen from Table 2 that the addition of 10^{-2} M of KI, KSCN, and KBr inhibits the corrosion of zinc to a large extent, and by increasing the concentration of benzaldehyde derivatives (1×10^{-6} to 11×10^{-6} M), the percentage inhibition increases. This can be interpreted according to Fouda et al. (Ref 24), who proposed two types of joint adsorption, namely, competitive and cooperative. In the case of competitive adsorption, the anions and cations are adsorbed at different sites on the electrode surface, and in the case of cooperative adsorption, the anions are chemisorbed on the electrode surface, and the cations are adsorbed on a layer of the anion, apart from the adsorption on the surface directly.

From the data of Table 2 it is seen that KI would be considered as one of the effective anions for synergistic action with respect to the investigated salts. The net increment of inhibition efficiency shows a synergistic effect of KI, KSCN, and KBr with benzaldehyde derivatives. The synergistic effect depends on the type and concentration of anions. The inhibition efficiency in the presence of these anions decreases in the following order: KI > KSCN > KBr .The experimental results suggest that the presence of these anions in the solution stabilizes the adsorption of benzaldehyde derivatives on the metal surface and improves the inhibition efficiency of these derivatives.

Table 2 Data from mass loss of zinc dissolution in 0.5 M HCl at different concentrations of the benzaldehyde derivatives with additions of 1×10^{-2} M KI, KSCN, and KBr at 30 °C

Concentration, M	%In								
	KI			KSCN			KBr		
	(I)	(II)	(III)	(I)	(II)	(III)	(I)	(II)	(III)
1×10^{-6}	74.7	71.7	67.1	73.1	70.0	64.4	70.7	68.5	61.4
3×10^{-6}	76.3	72.3	68.9	73.6	71.6	65.2	72.2	69.4	62.7
5×10^{-6}	78.0	74.2	68.6	75.4	72.5	66.0	73.8	70.2	63.5
7×10^{-6}	80.4	75.0	70.3	76.6	73.2	67.6	75.4	70.9	64.3
9×10^{-6}	82.2	76.5	71.3	79.7	74.2	68.6	77.2	71.7	66.2
11×10^{-6}	83.2	77.3	73.4	82.5	75.1	70.3	79.1	73.7	67.9

The synergistic inhibition effect was evaluated using the parameter, S_θ, obtained from the surface coverage θ (measured from the mass-loss method) of the anion, cation, and both. Aramaki and Hackerman (Ref 25) calculated the synergistic parameter using the following equation:

$$S_\theta = (1 - \theta_{1+2})/(1 - \theta'_{1+2}) \quad \text{(Eq 5)}$$

where $\theta_{1+2} = \theta_1 + \theta_2 - \theta_1\theta_2$; θ'_{1+2} is the measured surface coverage by the anion in combination with cation; and θ_1 and θ_2 are the surface coverages by the anions and cations, respectively.

Table 3 lists the variation of the synergistic parameter (S_θ) in the presence of different concentrations of benzaldehyde derivatives. It is seen that all the values of S_θ are equal to nearly unity, and, therefore, the adsorption of each compound antagonizes the other's adsorption. Thus, benzaldehyde derivatives significantly improved the coverage, and, thus, also the quality and the inhibition efficiency of benzaldehyde derivatives on the corroding zinc.

It is also known that Zn surface has positive charge due to ($E_{corr} - E_{q=0} = \phi$), where ϕ is referred to as Antropov's rational potential or potential on the corrosive scale, and $E_{q=0}$ is the potential of zero charge. If ϕ is negative, then the electrode surface has net negative charge, and the absorption of cationic species is favored. If the adsorption of anions is favored, then ϕ must be positive. Thus, it is difficult for the positively charged benzaldehyde derivatives to approach the positively charged Zn surface because of the electrostatic repulsion. Therefore, these derivatives cannot act as excellent inhibitors for Zn corrosion in 0.5 M HCl solution without anions. In the presence of I^-, SCN^-, and Br^- ions, these anions get adsorbed on Zn surface, making the surface become negatively charged by means of electrostatic attraction following which protonated benzaldehyde derivatives easily reach the surface of Zn metal.

3.3 Adsorption Isotherm

Assuming that the corrosion inhibition was caused by the adsorption of aldehydes derivatives, the values of surface coverages for different concentrations of inhibitors in 0.5 M HCl were evaluated from mass-loss measurement using the following equation:

$$\theta = [(M_{free} - M_{inh})/M_{free}] \quad \text{(Eq 6)}$$

It was found that the values of (θ) increased with increasing concentration of benzaldehydes derivatives. Using these values of surface coverage, one can utilize different adsorption isotherms to interpret the experimental data. Plots of θ versus log C (Temkin's isotherm) for the adsorption of aldehyde derivatives on the surface of Zn in 0.5 M HCl are shown in Fig. 2. The data produced straight lines indicating that Temkin's isotherm is valid for this system. The values of free

Table 3 Synergism parameter (S_θ) for different concentrations of the organic additives with addition of 1×10^{-2} M KI

Corrosive medium	Concentration, M:	Synergism parameter (S_θ)					
		1×10^{-6}	3×10^{-6}	5×10^{-6}	7×10^{-6}	9×10^{-6}	11×10^{-6}
0.5 M HCl	(I)	0.94	0.94	0.93	0.95	0.92	0.94
	(II)	0.98	0.95	0.95	0.97	0.94	1.00
	(III)	0.96	0.93	0.96	0.93	1.00	1.00

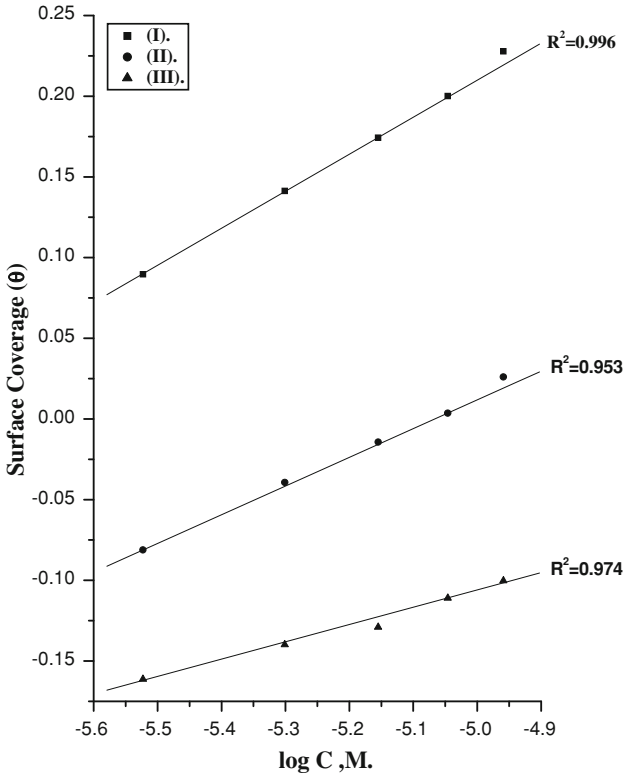

Fig. 2 Curve fitting of corrosion data for zinc in 0.5 M HCl in the presence of different concentrations of benzaldehyde derivatives to the Temkin's adsorption isotherm at 30 °C

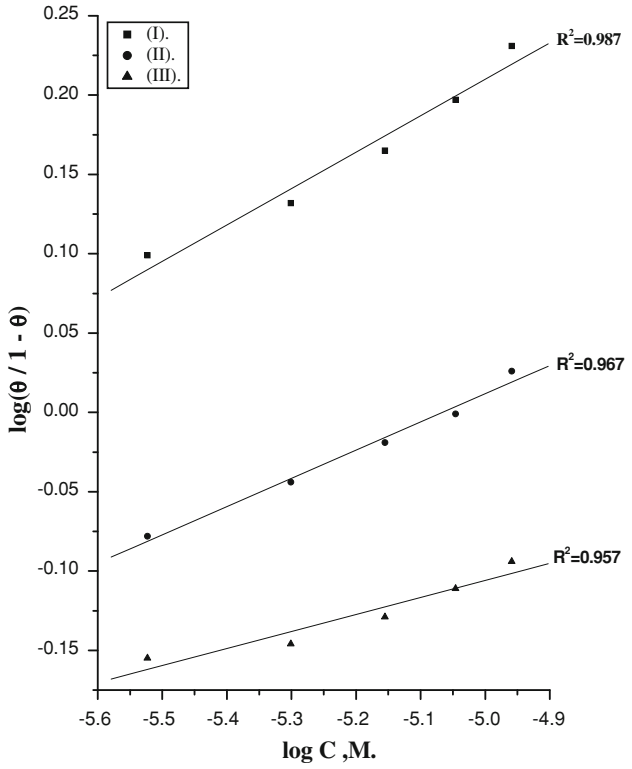

Fig. 3 Curve fitting of corrosion data for zinc in 0.5 M HCl in the presence of different concentrations of benzaldehyde derivatives to the kinetic model at 30 °C

Table 4 Inhibitor-binding constant (K), Free energy of binding, ΔG°_{ads}, the number of active sites ($1/y$), and later interaction parameter (a) for organic additives at 30 °C

		Kinetic model			Temkin		
Corrosive medium	Inhibitors	$1/y$	$K \times 10^{-4}$ M^{-1}	$-\Delta G^{\circ}_{ads}$, kJ mol^{-1}	a	$K \times 10^{-4}$ M^{-1}	$-\Delta G_{ads}$, kJ mol^{-1}
0.5 M HCl	(I)	5.3	2.8	42.2	10.5	2.7	45.2
	(II)	6.7	1.3	37.3	14.6	1.2	38.5
	(III)	10.0	1.0	32.1	22.5	1.1	34.2

energy of adsorption (ΔG°_{ads}) were calculated using the following equation:

$$K = 1/55.5 \exp\left[-\Delta G^{\circ}_{ads}/RT\right] \quad \text{(Eq 7)}$$

where K is the equilibrium constant, R is the universal gas constant, T is the absolute temperature, and 55.5 represents the concentration of water in mol L^{-1}.

On the other hand, it is found that the kinetic-thermodynamic model of El-Awady and Ahmed (Ref 26) which has the formula:

$$\log(\theta/1-\theta) = \log K' - y \log C \quad \text{(Eq 8)}$$

is valid to operate the present adsorption data. The equilibrium constant of adsorption, $K = K'^{(1/y)}$, where $1/y$ is the number of the surface-active sites occupied by one benzaldehyde molecule, and C is the bulk concentration of the inhibitor. By plotting [log $(\theta/1-\theta)$] versus C at 30 °C, a linear relationship was obtained (Fig. 3) suggestive of the validity of this model for all the cases studied. The calculated values of $1/y$, K, and ΔG°_{ads} are given in Table 4; On an inspection of these data, it is noted that ΔG°_{ads} values have a negative sign, indicating that the adsorption process proceeds spontaneously, and they increase as the percentage inhibition increases.

3.4 Effect of temperature

The effect of Temperature (30-55 °C) on the corrosion of zinc electrode in 0.5 M HCl in the presence of different concentrations of inhibitors was studied using mass-loss measurements. Similar curves to Fig 1 were obtained (not shown) .As the temperature increases, the rate of corrosion increases and hence the inhibition efficiency of the additives decreases .This is because desorption is aided by increasing the temperature. This behavior proves that the adsorption of inhibitors on the zinc surface occurs through physical adsorption.

Activation parameters for corrosion of zinc were calculated from Arrhenius-type plot.

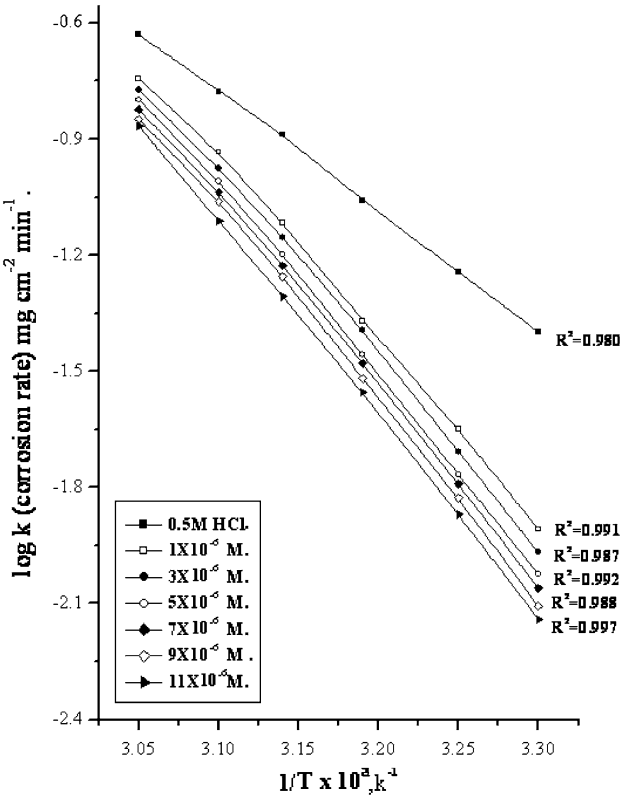

Fig. 4 log k (corrosion rate) – $1/T$ curves for zinc dissolution in 0.5 M HCl in the absence and the presence of different concentrations of inhibitor (I)

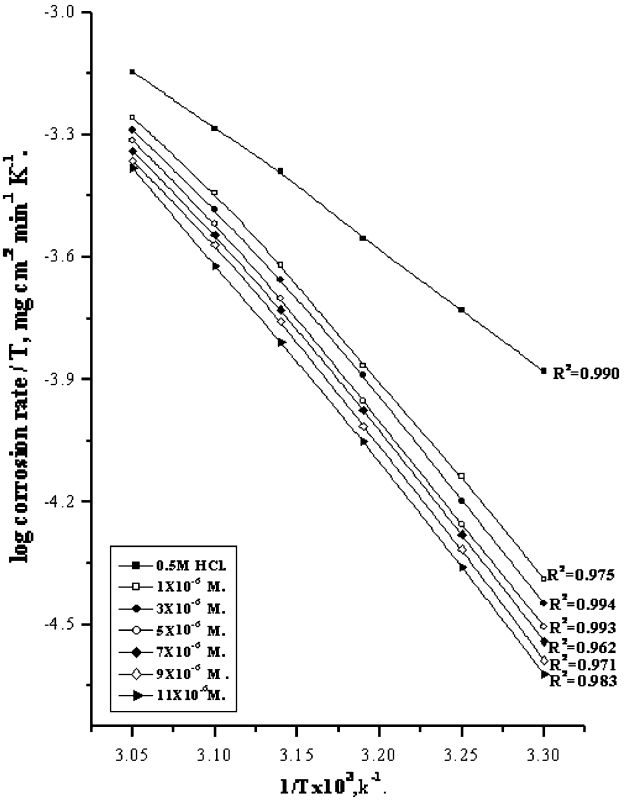

Fig. 5 log (corrosion rate/T) – ($1/T$) curves for zinc dissolution in 0.5 M HCl in the absence and the presence of different concentrations of inhibitor (I)

Table 5 Activation parameters for the dissolution of zinc in the presence and the absence of different concentrations of inhibitors in 0.5 M HCl

Inhibitor	Concentrations, M	Activation parameters		
		E_a^*, kJ mol^{-1}	ΔH^*, kJ mol^{-1}	$-\Delta S^*$, J mol^{-1} K^{-1}
Free acid (0.5 M HCl)	0	42.2	21.1	51.2
(I)	1×10^{-6}	55.0	56.2	7.6
	3×10^{-6}	63.4	59.5	8.9
	5×10^{-6}	65.1	61.1	10.2
	7×10^{-6}	65.2	62.1	11.7
	9×10^{-6}	66.3	63.0	13.4
	11×10^{-6}	67.0	64.1	14.9
(II)	1×10^{-6}	40.0	46.8	8.2
	3×10^{-6}	43.1	48.3	10.7
	5×10^{-6}	45.2	50.5	11.9
	7×10^{-6}	46.6	51.3	14.1
	9×10^{-6}	48.2	52.5	17.5
	11×10^{-6}	50.2	53.4	22.0
(III)	1×10^{-6}	37.7	41.4	13.4
	3×10^{-6}	39.4	41.9	17.6
	5×10^{-6}	43.0	44.0	27.5
	7×10^{-6}	44.0	45.3	31.1
	9×10^{-6}	44.3	49.3	31.4
	11×10^{-6}	45.6	50.2	34.2

$$k = A \exp\left(-E_a^*/RT\right) \quad \text{(Eq 9)}$$

and transition state-type equation:

$$k = RT/Nh \exp(\Delta S^*/R) \exp(-\Delta H^*/RT) \quad \text{(Eq 10)}$$

where k is the rate of metal dissolution, A is the frequency factor, N is Avogadro's number, R is the universal gas constant, h is Planck's constant, T is the absolute temperature, ΔH^* is the activation enthalpy, and ΔS^* is the activation entropy.

Figure 4 represents a plot of log k (corrosion rate) against $1/T$ (absolute temperature) for zinc in 0.5 M HCl solution in the absence and in the presence of different concentrations of the compound (I). Similar curves were obtained for other compounds (not shown). Straight lines were obtained with the slope of $-E_a^*/2.303R$. The value of activation energy was found to be 42.2 kJ mol^{-1} for 0.5 M HCl, which is above the value for the acid containing inhibitors (Table 5). On other hand, Fig. 5 illustrates the plots of log k/T versus $1/T$ for zinc electrode in 0.5 M HCl solution in the absence and the presence of different concentrations of compound (I). Similar curves were obtained for the other compounds (not shown). From the slopes of these lines, ΔH^* values can be computed, and from their intercepts, ΔS^* also can be computed.

The calculated values of the apparent activation energies E_a^*, the activation enthalpies ΔH^*, and the activation entropies ΔS^* for zinc dissolution in 0.5 M HCl solution in the absence and

the presence of different additives are shown in Table 5. The presence of benzaldehyde derivatives increases the activation energies of zinc indicating strong adsorption of the inhibitor molecules on the metal surface, and the presence of these additives induces energy barrier for the corrosion reaction, with this barrier increasing with increasing additive concentrations.

The results of Table 5 show that the enthalpies of activation are positive. The positive sign of enthalpy reflects the endothermic nature of the zinc dissolution process (Ref 27). Also, all the values of the entropies of activation are negative, implying that the activated complex is the rate-determining step and represents an association, rather than a dissociation, step meaning that a decreasing order takes place while transiting from the reactants to the activated complex (Ref 28).

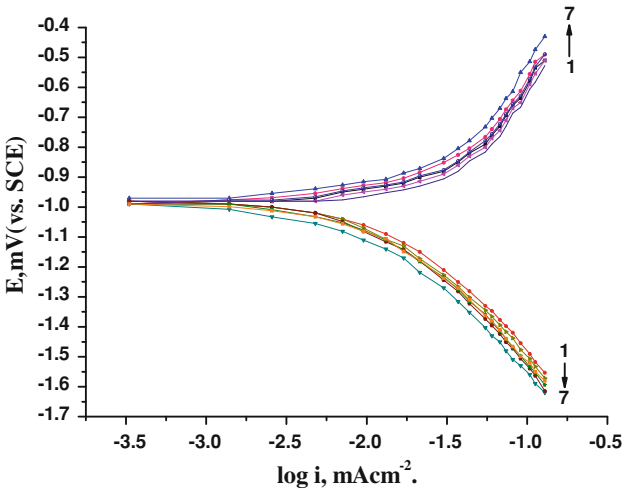

Fig. 6 Potentiodynamic polarization curves of zinc electrode in 0.5 M HCl solution in the absence and the presence of different concentrations of compound (I) at scan rate 10 mV s^{-1}: (1) 0.00 M compound I, (2) 1×10^{-6}, (3) 3×10^{-6}, (4) 5×10^{-6}, (5) 7×10^{-6}, (6) 9×10^{-6}, and (7) 11×10^{-6} M

3.5 Potentiodynamic Polarization Measurement

The effect of addition of some of the benzaldehyde derivatives on the potentiodynamic polarization curves of zinc in 0.5 M HCl solution at 25 °C with the scan rate of 10 mV s^{-1} was studied. The effect of increased concentration of compound I is represented as an example in Fig. 6. Similar curves were obtained for the other two compounds (not shown), but the corrosion parameters obtained are listed in Table 6. One can immediately observe that there is a transition region in which the potential increases (anodic polarization) or decreases (cathodic polarization) slowly with current density followed by a rapid linear build up of potential with current density (Tafel region).

Table 6 shows the effect of additive's concentration on the corrosion kinetic parameters, such as corrosion potential (E_{corr}), corrosion current density (I_{corr}), cathodic and anodic Tafel slopes (β_a and β_c), surface coverage (θ) and inhibition efficiency (%In), obtained from potentiodynamic polarization measurements at 25 °C.

Table 6 reveals that the increasing concentration of the additives leads to the following: The values β_c and β_a are almost constant to the blank curve. This means that these compounds influence Tafel slopes. However, the data suggested that these compounds act mainly as mixed-type inhibitors with a slight predominance of cathodic character due the shift of E_{corr} to more negative potential. The value of I_{corr} decreases, indicating the inhibiting effect of these compounds. These values of percentage of inhibition efficiency of the three tested compounds decrease in the following order: Compound I > Compound II > Compound III.

3.6 Electrochemical Impedance Spectroscopy

Impedance diagrams (Nyquist plots) at frequencies ranging from 1 Hz to 1 kHz with 10 mV amplitude signal at OCP for zinc in 0.5 M HCl in the absence and the presence of different concentrations of compounds (I-III) are obtained. The equivalent circuit that describes the metal/electrolyte interface is

Table 6 Corrosion parameters of Zn electrode in 0.5 M HCl solution containing different concentrations of inhibitors:

Inhibitor	Concentration, M	$-E_{corr}$, mV vs. SCE	I_{corr}, mA cm^{-2}	β_c, mV dec^{-1}	β_a, mV dec^{-1}	θ	%In
Free acid (0.5 M HCl)	0	990	198	412	505	…	…
(I)	1×10^{-6}	991	140	415	508	0.293	29.29
	3×10^{-6}	993	132	420	513	0.333	33.33
	5×10^{-6}	994	126	424	518	0.363	36.36
	7×10^{-6}	993	119	430	520	0.399	39.89
	9×10^{-6}	996	112	435	525	0.434	43.43
	11×10^{-6}	996	104	440	530	0.475	47.47
(II)	1×10^{-6}	994	146	422	512	0.263	26.26
	3×10^{-6}	995	138	428	518	0.303	30.30
	5×10^{-6}	997	130	430	524	0.343	34.34
	7×10^{-6}	999	125	435	530	0.369	36.86
	9×10^{-6}	995	118	440	538	0.404	40.40
	11×10^{-6}	999	108	448	544	0.455	45.45
(III)	1×10^{-6}	993	150	425	518	0.242	24.24
	3×10^{-6}	991	142	433	524	0.283	28.28
	5×10^{-6}	993	135	438	530	0.318	31.82
	7×10^{-6}	995	130	445	535	0.343	34.34
	9×10^{-6}	996	122	450	542	0.384	38.38
	11×10^{-6}	998	115	455	552	0.419	41.91

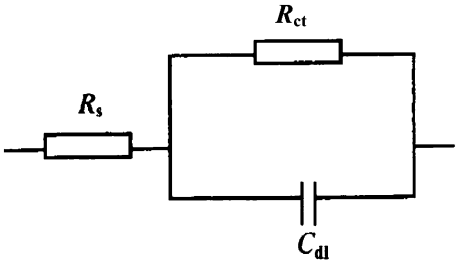

Fig. 7 Equivalent circuit of Randles cell

Table 7 Electrochemical kinetic parameter obtained by EIS technique for the corrosion of Zn in 0.5 M HCl at different concentrations of compounds at 25 °C

Inhibitor	Concentration, M	C_{dl}, μF cm^{-2}	R_{ct}, Ω cm^2	θ	%In
Free acid (0.5 M HCl)	0	59.62	3.99	0	0
(I)	3×10^{-6}	59.6	5.6	0.304	30.46
	7×10^{-6}	56.98	6.1	0.363	36.32
	9×10^{-6}	49.86	6.9	0.423	42.3
	11×10^{-6}	47.17	7.9	0.499	49.9
(II)	3×10^{-6}	59.17	5.5	0.292	29.29
	7×10^{-6}	53.16	6	0.316	35.16
	9×10^{-6}	44.95	6.9	0.422	42.2
	11×10^{-6}	44.86	7.24	0.449	44.9
(III)	3×10^{-6}	57.08	5.41	0.281	28.12
	7×10^{-6}	41.95	5.88	0.335	33.59
	9×10^{-6}	39.24	6.61	0.396	39.6
	11×10^{-6}	37.03	7.24	0.449	44.9

shown in Fig. 7, where R_s, R_{ct}, and CPE refer to the solution resistance, the charge transfer resistance, and the constant phase element, respectively. EIS parameters and %In are calculated and tabulated in Table 7. In order to correlate impedance and polarization methods, I_{corr} values are obtained from polarization curves, and Nyquist plots in the absence and the presence of different concentrations of compounds (I-III) using the Stern-Geary equation:

$$I_{corr} = \frac{\beta_a \beta_c}{2.303(\beta_a + \beta_c)R_{ct}} \quad \text{(Eq 11)}$$

The obtained Nyquist plot for compound (I) is shown in Fig. 8. Each spectrum is characterized by a single, full semicircle. The fact that impedance diagrams have an approximately semicircular appearance shows that the corrosion of zinc is controlled by a charge transfer process. Small distortion is observed in some diagrams, which has been attributed to frequency dispersion (Ref 29, 30). The diameter of the capacitive loop obtained increases in the presence of benzaldehyde derivatives, and this increase in the diameter is indicative of the degree of inhibition of the corrosion process.

It is observed from the obtained EIS data that R_{ct} increases, and C_{dl} decreases with the increasing inhibitor concentration. The increase in R_{ct} values, and consequently of inhibition efficiency, may be due to the gradual replacement of water molecules by the adsorption of the inhibitor molecules on the metal surface to form an adherent film on the metal surface, and this suggests that the coverage of the metal surface by the film decreases the double-layer thickness. Also, this decrease of C_{dl}

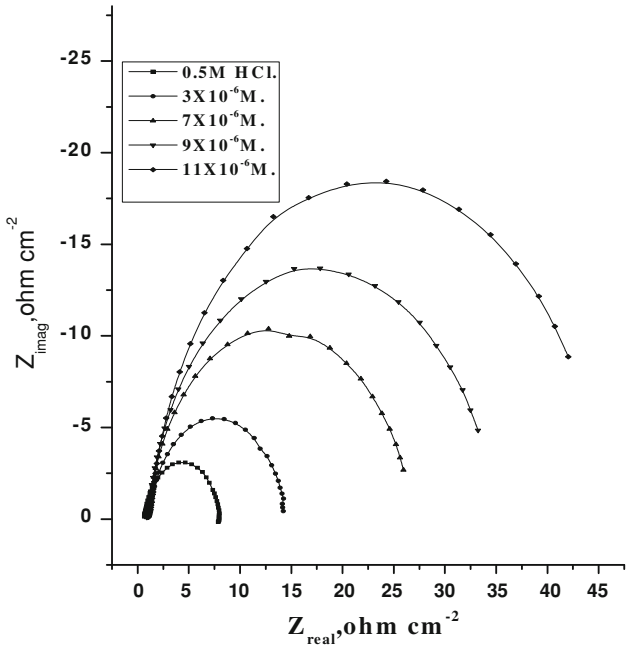

Fig. 8 Nyquist plots for zinc in 0.5 M HCl solution in the absence and the presence of different concentrations of compound (I)

at the metal/solution interface with increasing inhibitor concentration can result from a decrease in local dielectric constant, indicating that the inhibitors were adsorbed on the surface at both anodic and cathodic sites. The impedance data confirm the inhibition behaviors of the inhibitors obtained using other techniques. From the data of Table 7, it is seen that the I_{corr} values decrease significantly in the presence of these additives and that the %In is greatly improved. The order of reduction in I_{corr} exactly correlates with that obtained from potentiodynamic polarization studies. Moreover, the decrease in the values of I_{corr} follows the same order as that obtained for the values of C_{dl}. It can be concluded that the inhibition efficiency found from weight loss, polarization curves, EIS measurements, and the Stern-Geary equation are all in good agreement.

3.7 Mechanism of the Action of Inhibitors

Inhibitors are mainly organic compounds with at least one polar unit having atoms of sulfur, nitrogen, oxygen, phosphorous, and selenium. The polar unit acts as the reaction center. The organic compounds which act as inhibitors (R_nX) are adsorbed on the surface of the metal, M, forming a charge transfer bond between their polar atoms and the metal:

$$M + R_nX: \rightleftarrows M{:}XR_n \quad \text{(Eq 12)}$$

The number of adsorption active sites and their charge densities, their molecular sizes, shapes, and orientations determine the degree of adsorption, and hence the effectiveness of the inhibitors.

The order of the decrease in the inhibition efficiency of benzaldehyde derivatives occurs in the following sequence: (I) > (II) > (III).

Compound (I) exhibits excellent inhibition efficiency because of the presence of two OH groups which are more basic and one OH group present in the para position has Hammett constant ($\sigma = -0.37$) but compound (II) has two CH_3 groups which are less basic than OH group and CH_3 group in

the para position has Hammett constant ($\sigma = -0.17$) which is less than OH group, in addition compound (I) has larger molecular size than compound (II) so compound (I) is more efficient than compound (II). Compound (III) is the least efficient due to the absence of any substituted group in para position. Compounds I, II may form complex with Zn ions, and this complex may be adsorbed on the Zn surface.

4. Conclusions

1. Benzaldehyde derivatives have been used for inhibiting the corrosion of Zn in 0.5 M HCl.
2. The potentiodynamic polarization data indicate that these are mixed-type inhibitors.
3. The investigated benzaldehyde derivatives are adsorbed on Zn surface following Temkin's isotherm model.
4. Adsorption ability and inhibition efficiency reduce with increment of temperature.
5. Because, both -CH_3 and -OH groups activate the benzene ring, and so compounds (I) and (II) behave as efficient inhibitors, in compound (III); the presence of -OH in the ortho position would facilitate the formation of a chelate having a five-membered ring.

References

1. G.W. Waltter, Corrosion Rates of Zinc, Zinc Coatings and Steel in Aerated Slightly Acidic Chloride Solutions Calculated from Low Polarization Data, *Corros. Sci.*, 1976, **16**, p 573–586
2. L. Wang, J.-X. Pu, and H.-C. Luo, Corrosion Inhibition of Zinc in Phosphoric Acid Solution by 2-Mercaptobenzimidazole, *Corros. Sci.*, 2003, **45**, p 677–683
3. S.A. Odomelam, E.C. Ogoko, B.I. Ito, and N.O. Eddy, Adsorption and Inhibitive Properties of Clarithromycin for the Corrosion of Zn in 0.01 to 0.05 M H_2SO_4, *Portugal. Electrochim. Acta*, 2009, **27**(1), p 57–68
4. Y.K. Agrawal, J.D. Talati, M.D. Shah, M.N. Desai, and N.K. Shah, Schiff Bases of Ethylenediamine as Corrosion Inhibitors of Zinc in Sulphuric Acid, *Corros. Sci.*, 2004, **46**, p 633–651
5. M.S. Abdal-Aal, Z.A. Ahmed, and M.S. Hassan, Inhibiting and Accelerating Effects of Some Quinolines on the Corrosion of Zinc and Some Binary Zinc Alloys in HCl Solution, *J. Appl. Electrochem.*, 1992, **22**, p 1104–1109
6. O.K. Abiola and A.O. James, The Effect of Aloe Vera Extract on Corrosion and Kinetics of Zinc in HCl Solution, *Corros. Sci.,* 2010**,** **52**(2), p 661–664
7. M. Abdallah, A.Y. El-Etre, and M.F. Moustafa, Amidopoly Ethylamines as Corrosion Inhibitors for Zinc Dissolution in Different Acidic Electrolyte, *Portugal. Electrochim. Acta*, 2009, **27**(5), p 615–630
8. A.Y. El-Etre, M. Abdallah, and Z.E. El-Tantawy, Corrosion Inhibition of Some Metals Using Lawasonia Extract, *Corros. Sci.*, 2005, **47**, p 385–395
9. M. Abdallha, Ethoxylate Fatty Alcohols as Corrosion Inhibitor for Dissolution of Zinc in Hydrochloric Acid, *Corros. Sci.*, 2003, **45**, p 2705–2716
10. E.E. Foad El-Sherbini, S.M. Abd El-Wahab, and M. Deyab, Ethoxylated Fatty Acids as Inhibitors for the Corrosion of Zinc in Acid Media, *Mater. Chem. Phys.*, 2005, **89**(2–3), p 183–191
11. A.A. Abdel Fattah, E.M. Mabrouk, Abd EL-Gulil, and M.M. Ghoneim, N-Hetrocyclic Compound as Corrosion Inhibitors for Zn in HCl Acid Solutions, *Bull. Soc. Chim. Fr.*, 1991, **127**, p 48–53
12. M.N. Desai, J.D. Talati, and N.K. Sheh, Schiff Bases of Ethylenediamine/Triethylenetetramine with Benzaldehyde/Cinnamic Aldehyde/Salicylaldehyde as Corrosion Inhibitors of Zinc in Sulphuric Acid, *Anti-Corros. Methods Mater.*, 2008, **55**(1), p 27–37
13. M. Abdallah, A.Y. El-Etre, and M.F. Moustafa, Effect of Some Amidopoly Ethylamine on Corrosion of Zinc Electrode Used in Zinc-Manganese Batteries, *Prot. Met. Phys. Chem. Surf.*, 2011, **47**(2), p 246–252
14. A.S. Fouda, A.H. Elasklany, and L.H. Madkour, The Effect of Some β-Diketo Compounds on the Corrosion of Zinc in Hydrochloric Acid Solution, *Indian J. Chem. Soc.*, 1984, **61**, p 425–429
15. A.S. Fouda and L.H. Madkour, Inhibitive Action of Some Amines, Hydrazines Towards Corrosion of Zinc in Trichloroacetic Acid Solution, *Bull. Soc. Chim. France*, 1986, **5**, p 745–749
16. A.S. Fouda, A.K. Mohamed, H.A. Mostafa, and E.M. Hussein, A Study of the Inhibiting Action of Some Monosaccharides on the Corrosion of Zinc in HNO_3, *J. Indian Chem. Soc.*, 1989, **66**, p 417–419
17. A.S. Fouda, L.H. Madkour, A.A. El-Shafei, and S.A. Maksoud, Corrosion Inhibitors for Zinc in 2 M HCl Solution, *Korean Chem. Soc.*, 1995, **16**(5), p 454–458
18. A.S. El-Gaber, A.S. Fouda, and A.M. El-Desoky, Synergistic Inhibition of Zn Corrosion by Some Anions in Aqueous Media, *Ciencia Tecnologia dos Materiais*, 2008, **20**(3/4), p 71–77
19. A.S. Fouda, M. Abdallah, S.T. Atwa, and M.M. Salem, Tetrahydrocarbazole Derivatives as Corrosion Inhibitors for Zn in HCl Solution, *Mod. Appl. Sci.*, 2010, **4**(12), p 41–55
20. E.S. Lisac and S. Podbrscek, Non-toxic Organic Zinc Corrosion inhibitors in Hydrochloric Acid, *J. Appl. Electrochem.*, 1994, **24**, p 779–784
21. S.L. Granese, B.M. Rosales, C. Oviedo, and J.O. Zerbino, The Inhibition Action of Heterocyclic Nitrogen Organic Compounds on Fe and Steel in HCl Media, *Corros. Sci.*, 1992, **33**, p 1439–1453
22. I.L. Rosenfeld, *Corrosion Inhibitors*, McGraw-Hill, New York, 1981
23. V.R. Saliyan and A.V. Adhikari, Quinolin-5-ylmethylene-3-{[8-(trifluoromethyl)quinolin-4-yl]thio}propanohydrazide as an Effective Inhibitor of Mild Steel Corrosion in HCl Solution, *Corros. Sci.*, 2008, **50**(1), p 55–61
24. A.S. Fouda, M. Abdallah, and A. Attia, Inhibition of Carbon Steel Corrosion by Some Cyanoacetohydrazide Derivatives in HCl Solution, *Chem. Eng. Commun.*, 2010, **197**(8), p 1091–1108
25. K. Aramaki and N. Hackerman, Inhibition Mechanism of Medium-Sized Polymethyleneimine, *J. Electrochem. Soc.*, 1969, **116**, p 568–574
26. Y.A. El-Awady and S.A.I. Ahmed, Effect of Temperature and Inhibitor on the Corrosion of Four Primary Aliphatic Amines on Mild Steel in 2 M HCl Solution, *J. Ind. Chem.*, 1985, **24**, p 601–607
27. A.S. Fouda and A.S. Ellithy, Inhibition Effect of 4-Phenylthiazole Derivatives on Corrosion of 304 L Stainless Steel in HCl Solution, *Corros. Sci.*, 2009, **51**, p 868–875
28. S.M.A. Hosseini, M. Salari, E. Jamalizadeh, S. Khezripoor, and M. Seifi, Inhibition of Mild Steel Corrosion in Sulfuric Acid by Some Newly Synthesized Organic Compound, *Mater. Chem. Phys.*, 2010, **119**(1–2), p 100–105
29. E.E. Mccafferty, On the Determination of Distributed Double-Layer Capacitances from Cole-Cole Plots, *Corros. Sci.*, 1997, **39**(2), p 243–254
30. F. Mansfeld, S.L. Jeanjaquet, and M.W. Kendig, An Electrochemical Impedance Spectroscopy Study of Reactions at the Metal Interface, *Corros. Sci.*, 1986, **26**(9), p 735–742